



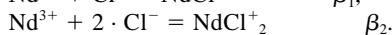
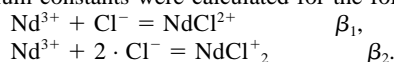
A spectrophotometric study of neodymium(III) complexation in chloride solutions

ART A. MIGDISOV and A. E. WILLIAMS-JONES*

Department of Earth and Planetary Sciences, McGill University, Montreal, PQ H3A 2A7, Canada

(Received January 24, 2002; accepted in revised form June 7, 2002)

Abstract—The formation constants of neodymium complexes in chloride solutions have been determined spectrophotometrically at temperatures of 25 to 250°C and a pressure of 50 bars. The simple ion, Nd^{3+} , is dominant at 25°C, whereas NdCl^{2+} and NdCl_2^+ are the dominant species at elevated temperatures. Equilibrium constants were calculated for the following reactions:



The values of β_1 were found to be identical within experimental error to the values reported by Gammons et al. (1996) but substantially different from those proposed by Stepanchikova and Kolonin (1999). The values of β_2 obtained in this study agree relatively well with those of Gammons et al. (1996); differences are greatest at intermediate temperature and reach a maximum of one half an order of magnitude at 200°C.

Theoretical estimates of β_1 and β_2 by Haas et al. (1995) using the revised Helgeson-Kirkham-Flowers (HKF) equation of state predict lower stability of NdCl^{2+} and NdCl_2^+ at temperatures above 150°C than determined in this study. A new fit to the HKF equation of state is therefore proposed, which yields values for β_1 and β_2 similar to those obtained experimentally.

Using the formation constants reported in this study, we predict that typical seafloor hydrothermal vent fluids will contain a maximum concentration of Nd of ~2 ppb. This value is several orders of magnitude lower than would be required to explain the levels of Nd mobility commonly reported for seafloor hydrothermal systems and suggests that other ligands may be more important than Cl in transporting rare earth elements in the Earth's crust. Copyright © 2002 Elsevier Science Ltd

1. INTRODUCTION

Hydrothermal transport is an important part of the geochemistry of rare earth elements (REEs), as shown by the enrichment of REEs during hydrothermal alteration (MacLean, 1988; Schandl and Gorton, 1991; Olivo and Williams-Jones, 1999), the presence of REE minerals such as bastnasite in fluid inclusions (Kwak and Abeysinghe, 1987; Salvi and Williams-Jones, 1990; Buhn and Rankin, 1999; Buhn et al., 1999; Vinokurov et al., 1999), and the occurrence of hydrothermal REE ore deposits (Drew et al., 1990; Smith and Henderson, 2000; Williams-Jones et al., 2000). This aspect of REE geochemistry is also of interest because the REEs may be used as surrogates for the actinides in studies of nuclear waste mobility (Wood, 1990; Wood and Ricketts, 2000). Unfortunately, our capacity to quantitatively model processes involving the hydrothermal transport of REEs is severely compromised by a lack of experimental data at elevated temperatures. Researchers have therefore had to resort to theoretical estimates based on data obtained at room temperature (Wood, 1990; Haas et al., 1995).

Experimental studies of the behavior of REEs in aqueous solutions at elevated temperature have been limited to their complexation with chloride (Gammons et al., 1996; Stepanchikova and Kolonin, 1999; Gammons et al., 2002) and acetate (Wood et al., 2000) ions. The experiments of Gammons et al. (1996) and Stepanchikova and Kolonin (1999) showed that Nd forms complexes with chloride that are significantly more stable than theoretically predicted. The subsequent study

by Gammons et al. (2002) confirmed this finding for solutions at 200°C and demonstrated that the other REEs form complexes with chlorides similar in stability to that of the Nd-chloride complexes; the earlier experiments by Gammons et al. (1996) on Nd-chloride complexation were not repeated in this study. These studies suggest that hydrothermal fluids may be capable of transporting significant concentration of the REEs as chloride complexes.

Unfortunately, the experimental data for Nd-chloride complexes referred to above cannot be applied with any confidence, because of the large disagreement in the values of formation constants recommended by the two studies. The goal of the present study was to resolve this disagreement by using an *in situ*, ultraviolet (UV)–visible spectroscopic method similar to that used by Stepanchikova and Kolonin (1999), which theoretically is more precise than the solubility method employed by Gammons et al. (1996).

2. METHOD

Experiments were conducted at a temperature of 25°C and at 25°C intervals from 100 to 250°C and a pressure of 50 bars using a high-temperature, flow-through, UV-visible spectroscopic system (Fig. 1). The cell was constructed from grade 4 titanium alloy using plans provided by T. Seward (ETH, Zurich, Switzerland) and was equipped with fused silica windows. The path length (0.98 cm) was determined by a calibration procedure involving measurements of the absorption of a 5×10^{-3} mol·dm⁻³ potassium iodide solution¹ in a standard 1-cm

* Author to whom correspondence should be addressed (artas@eps.mcgill.ca).

¹ Here and elsewhere, the concentrations are reported in molar units to reflect the manner in which the experimental solutions were prepared. These concentrations were later converted to molal (mol/kg⁻¹) units to evaluate the formation constants.

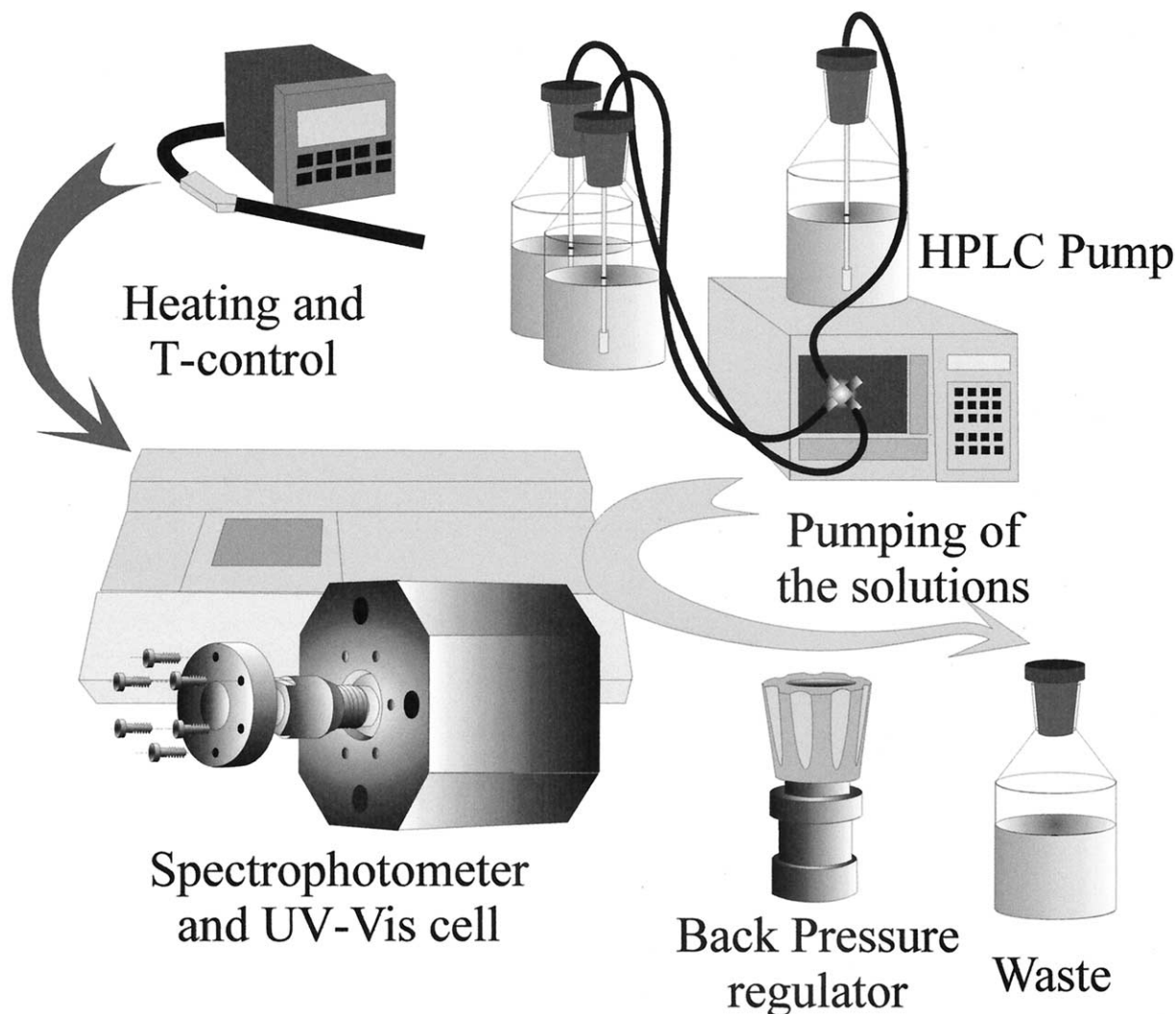


Fig. 1. The spectrophotometric high-temperature cell with the experimental setup used in this study.

quartz cuvette and in the flow-through cell at 25°C. The cell was heated using heating elements introduced into the cell body and the heating controlled by an Omega CN-2001 regulator, which permits the temperature of the experiment to be maintained within an error of $\pm 0.5^\circ\text{C}$. Pressure was controlled using a Hewlett-Packard 1050 HPLC pump and a Tescom 26-1762 back pressure regulator. Spectrophotometric measurements were made at 1-nm intervals over the range 200 to 900 nm using a Cary 100 double-beam spectrophotometer.

Absorption spectra were collected for 30 to 24 solutions (depending on the isotherm investigated; Table 1) with total Nd concentrations ranging from 2×10^{-4} to 5.18×10^{-2} mol·dm $^{-3}$ and total chloride concentrations from 1.7×10^{-2} to 1.9×10^{-1} mol·dm $^{-3}$. The solutions were prepared by dissolving Optima-grade hydrochloric acid (Fisher Scientific), REActon-grade neodymium(III) chloride (Alfa Aesar), and Puratronic-grade sodium chloride (Alfa Aesar) in Nanopure deionized water. The solutions were prepared to have a pH $^{25^\circ\text{C}}$ of 1.5. This pH $^{25^\circ\text{C}}$ was selected on the basis of exploratory experiments, which show that the Nd-Cl solutions with pH $^{25^\circ\text{C}} > 2.5$ produce spectra that are variably shifted to higher absorption values by comparison with spectra for more acidic solutions; the shift is tentatively attributed to hydrolysis at the temperatures of the experiments. Absorption spectra were also collected for eight chloride-free solutions having total concentrations of Nd $^{3+}$ ranging from 1.9×10^{-3} to 4.7×10^{-2} mol·dm $^{-3}$, which were prepared by dissolving REActon-grade neodymium(III) oxide (Alfa Aesar) and Optima-grade perchloric acid (Fisher Scientific)

in Nanopure deionized water. As in the case of the Nd-Cl solutions, the pH $^{25^\circ\text{C}}$ of the solutions was 1.5. The total Nd and Cl concentrations of the solutions were analyzed at Ecole Polytechnique (Montreal, Canada) using the neutron activation method. To correct the spectra for background absorption, the absorption of the cell filled with Nanopure deionized water was recorded before each of the Nd spectra was collected.

An estimate of the error of the measured absorption values was obtained by repeated measurements (several sets of 5 to 10 scans at each temperature) of the spectra of a solution having a total Nd concentration of 2×10^{-2} mol·kg $^{-1}$. It was found that the absorption values were reproducible to a tolerance (uncertainty in absolute units) that varied from 0.01 to 0.03, increasing with temperature and decreasing with wavelength.

3. RESULTS

The absorption spectra recorded for the perchloric acid solutions display several multiplets in the wavelength range of 320 to 900 nm, but no obvious peak was detected in the UV part of the spectrum. The spectra collected at 25°C are in good agreement with those of Carnall (1979) and with the electronic spectrum of the hydrated Nd $^{3+}$ ion calculated by Kotzian et al.

Table 1. The results of calculations for the absorption matrix at different temperatures and wavelength ranges. The rank represents the number of independent linear equations in the absorption matrix, which, effectively, is the number of absorbing species (see explanation in the text). The species listed are those interpreted to absorb at the wavelength range indicated. The species in parentheses are those not obviously present in the solution (see explanation in the text).

$T(^{\circ}\text{C})$	Wavelengths (nm)	Number of solutions	Rank	Absorbing species
25	310–900	30	2 (1)	Nd^{3+} , (NdCl_2^{2+})
100	310–900	27	3 (2)	Nd^{3+} , NdCl_2^{2+} , (NdCl_2^{+})
125	310–900	28	3	Nd^{3+} , NdCl_2^{2+} , NdCl_2^{+}
150	310–900	26	3	Nd^{3+} , NdCl_2^{2+} , NdCl_2^{+}
175	310–900	24	3	Nd^{3+} , NdCl_2^{2+} , NdCl_2^{+}
200	310–900	26	3	Nd^{3+} , NdCl_2^{2+} , NdCl_2^{+}
225	310–900	24	3	Nd^{3+} , NdCl_2^{2+} , NdCl_2^{+}
250	310–900	24	3	Nd^{3+} , NdCl_2^{2+} , NdCl_2^{+}
25	200–900	30	3 (2)	Nd^{3+} , (NdCl_2^{2+}) , Cl^{-}
100	210–900	27	4 (3)	Nd^{3+} , NdCl_2^{2+} , (NdCl_2^{+}) , Cl^{-}
125	210–900	28	4	Nd^{3+} , NdCl_2^{2+} , NdCl_2^{+} , Cl^{-}
150	215–900	26	4	Nd^{3+} , NdCl_2^{2+} , NdCl_2^{+} , Cl^{-}
175	218–900	24	4	Nd^{3+} , NdCl_2^{2+} , NdCl_2^{+} , Cl^{-}
200	225–900	26	4	Nd^{3+} , NdCl_2^{2+} , NdCl_2^{+} , Cl^{-}
225	228–900	24	4	Nd^{3+} , NdCl_2^{2+} , NdCl_2^{+} , Cl^{-}
250	230–900	24	4	Nd^{3+} , NdCl_2^{2+} , NdCl_2^{+} , Cl^{-}

(1995). Heating of the solutions resulted in a significant decrease of the absorption intensity, which is consistent with the findings of Stepanchikova and Kolonin (1999). However, the intensities of the absorption bands were found to be 20 to 50% weaker than those of Stepanchikova and Kolonin (1999). The differences are greatest in the near-UV region and decrease toward the infrared part of the spectrum.

A spectroscopic study of Nd^{3+} solutions at 25°C by Choppin et al. (1966) demonstrated that the perchloric ion cannot form spectroscopically detectable complexes with Nd at concentrations below $6 \text{ mol}\cdot\text{dm}^{-3}$. We therefore concluded that the only absorbing species in perchloric solutions at the wavelengths investigated is Nd^{3+} and that the absorbance recorded can be described by the following equation:

$$A = \varepsilon_{\text{Nd}^{3+}} \cdot M_{\text{Nd}^{3+}} \cdot l,$$

where A is absorbance, ε is the molar extinction coefficient (or molal absorption coefficient), l is the path length, and M is the molar concentration of Nd^{3+} ($\text{mol}\cdot\text{dm}^{-3}$). The data obtained for Nd^{3+} in the perchloric acid solutions at the different temperatures were expressed in the form of extinction coefficients and are illustrated in Figure 2.

The effect of temperature on the spectra of neodymium chloride solutions is illustrated in Figure 3. However, because of problems, which will be discussed below, the spectra have not been corrected for the chloride ion absorbance. As can be seen from this figure, heating the solutions resulted in a progressive red shift of the peak maxima and a decrease in absorption intensity. Examples of the isothermal spectra collected for a set of solutions with different Nd:Cl ratios are illustrated in Figure 4. Changes in the ratio do not result in the production of new maxima or modification of the peak shapes.

4. DATA TREATMENT

4.1. Speciation Model

We used the method of absorbance matrix analysis described by Suleimenov and Seward (2000) to develop a chemical

model for the solutions investigated and to determine the number of absorbing species. Assuming a conventional linear model with respect to chemical composition, each of the experimental measurements at a given wavelength can be represented as

$$\frac{A}{l} = \varepsilon_1 \cdot M_1 + \varepsilon_2 \cdot M_2 + \dots + \varepsilon_n \cdot M_n, \quad (1)$$

where A is absorbance, ε_n is the molar extinction coefficient (or molal absorption coefficient) of the corresponding species, l is the path length, and M_n is the molar concentration of the corresponding species. Because absorbance is a linear function of the composition of the solution, the maximum number of linearly independent columns in the absorbance matrix gives the number of absorbing species at the temperature investigated. If no two species have the same molar extinction coefficient, this number can be found by determining the rank of the absorbance matrix. The latter was calculated using MATLAB software, which employs a method based on the singular value decomposition (Dongarra et al., 1979). The absorption matrices used to evaluate the number of absorbing species were not corrected for the chloride ion absorbance, because in all of the solutions investigated, some significant but unknown amount of chloride ion was bound in neodymium complexes. Thus, the correction normally made by subtracting the spectrum for a chloride solution of corresponding concentration could not be applied to the systems investigated, because the concentrations of Cl^{-} are not sufficiently well known.

Because the experimentally determined uncertainties in the absorption values varied from 0.010 to 0.030 at 25 and 100°C and from 0.020 to 0.030 at higher temperatures, the results of the rank calculations for these tolerance intervals were taken as the total number of absorbing species. The results of the rank calculations are summarized in Table 1 and Figure 5a and show that for the isotherms investigated, excepting those for 25 and 100°C , the total number of absorbing species, including Cl^{-} , is four.

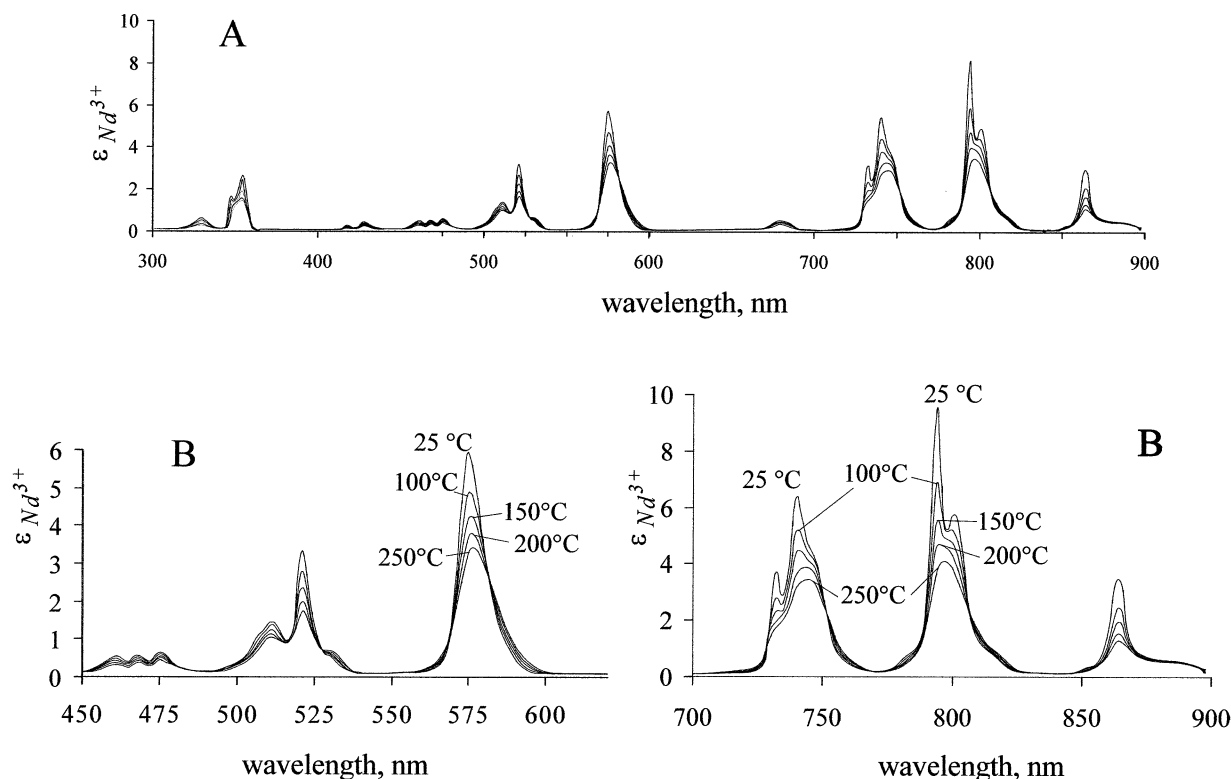


Fig. 2. (A) The molar extinction coefficients for Nd^{3+} measured in solutions with total concentrations of Nd^{3+} ranging from 1.9×10^{-3} to 4.7×10^{-2} mol-dm $^{-3}$ at temperatures of 25 to 250 °C ($l = 0.98$ cm). (B) Enlargements of parts of the spectra shown in (A).

The rank calculations were repeated for a reduced absorbance matrix (310 to 900 nm; Table 1, Fig. 5b), from which the absorbance of chloride ion was removed. In principle, this stripping of the matrix should reduce by at least one the number of absorbing species and more if some of the species have no absorbance bands in the visible region. The rank calculation for the reduced matrix indicated three absorbing species at temperatures above 100 °C compared with four species in the full matrix. Thus, we conclude that the solutions contained three Nd species at the conditions of our experiments.

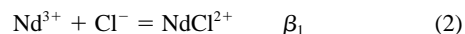
At a tolerance of 0.03, the rank of the reduced absorption matrix calculated for 25 and 100 °C was found to be equal to one and two, respectively, whereas at the tolerance range of 0.012 to 0.025 (0.027), the calculated rank was two and three, respectively. We therefore concluded that two and three absorbing Nd species, respectively, were present in the solutions investigated. However, as discussed below, the treatment of the spectra does not provide stable solutions for $\beta_1^{25^\circ C}$ and $\beta_2^{100^\circ C}$ (see Eqn. 2 and 3). We therefore concluded that $NdCl^{2+}$ and $NdCl_2^{+}$ at 25 °C and 100 °C, respectively, are present in detectable concentrations, but these concentrations are not high enough to permit accurate derivation of the corresponding formation constants. In view of the above, we treated our data with a four-species model, i.e., Nd^{3+} , $NdCl^{2+}$, $NdCl_2^{+}$, and Cl^- , except for data collected at 25 °C, for which a three-species model was employed (Nd^{3+} , $NdCl^{2+}$, and Cl^-).

The speciation model is the same as that proposed by Gammons et al. (1996) and differs from that of Stepanchikova and

Kolonin (1999), in which there are only two Nd species (Nd^{3+} and $NdCl^{2+}$). The disagreement with Stepanchikova and Kolonin (1999) is surprising considering that both studies were based on the UV-visible spectroscopic method and yielded similar raw data. However, the methods of data treatment were different. Whereas we used a mathematical analysis of the absorbance matrix to develop our model, Stepanchikova and Kolonin (1999) based their conclusions on the absence of isosbestic points in the isothermal spectra and a visual interpretation of peak shapes. Because isosbestic points are difficult to detect, especially if absorption bands are spaced closely and absorption intensities of the components differ in time, it seems likely that the visual method of analysis lacked the sensitivity required to adequately interpret the spectra of Nd-Cl solutions. We therefore believe that the ion species model first proposed by Gammons et al. (1996) provides the most reliable basis for interpreting the behavior of Nd in chloride solution at elevated temperature.

4.2. Calculation of the Formation Constants

Equilibrium constants were calculated for the following reactions:



and

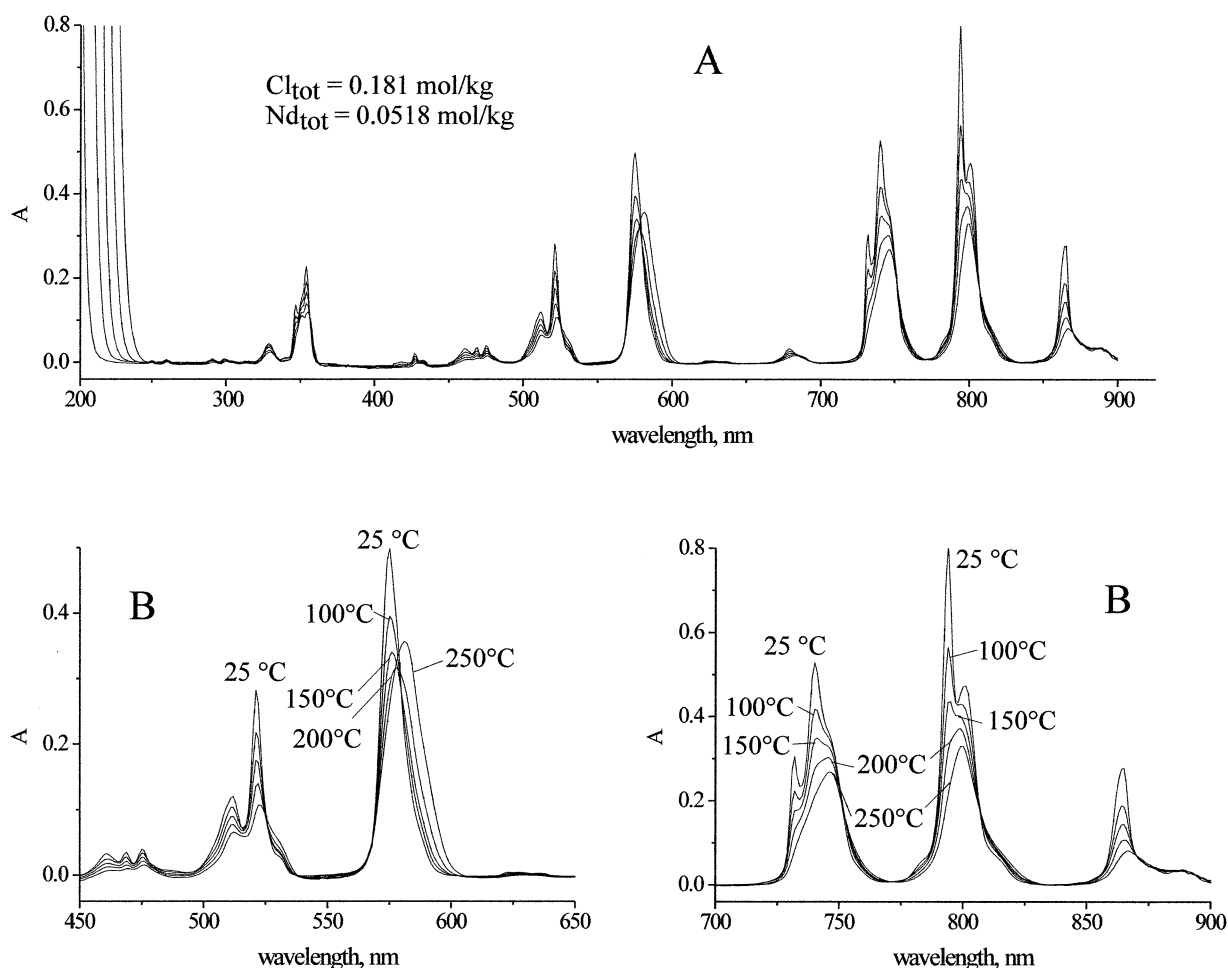
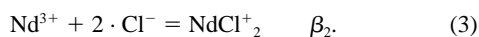


Fig. 3. (A) Examples of the spectra for neodymium chloride solution with a total concentration of neodymium of $0.0518 \text{ mol-dm}^{-3}$ and chloride ion of $0.181 \text{ mol-dm}^{-3}$ at temperatures ranging from 25 to 250°C (the measurements were made using a cell with a path length of 0.98 cm .) (B) Enlargements of parts of the spectra shown in (A).



Following the method described by Suleimenov and Seward (2000), the vector of equilibrium constants and the matrix of the molar extinction coefficients were determined via successive minimization of the following function:

$$U = \sum_{i=1}^I \left[\sum_{k=1}^K (A_{ik}^{obs} - A_{ik}^{calc})^2 \right] \quad (4)$$

where i identifies the wavelength, I is the total number of wavelengths at which measurements were made, and K is the number of solutions (for details, see Suleimenov and Seward, 2000). The calculations were performed using MATLAB software (function "fmins"); the algorithm employed in the minimization was the Nelder-Mead simplex search described by Nelder and Mead (1965) and Dennis and Woods (1987). Only wavelength intervals in which peaks were detected were considered in the calculations. A peak was interpreted when the difference between the background absorption and that of the solution reached 0.05 absorption units.

A schematic block diagram describing the algorithm used to calculate the formation constants is illustrated in Figure 6. The variable A_{ik}^{calc} is the calculated absorbance and is a function of the concentrations of Nd species and their molar extinction coefficients (see Eqn. 1). The equilibrium concentrations of Nd^{3+} , NdCl_2^+ , NdCl_2^+ , and Cl^- were calculated using initial guesses of the formation constants β_1 and β_2 and the total concentrations of Nd and Cl in the solutions investigated. The activity model used in the calculations was chosen to be identical to that used by Gammons et al. (1996) and is similar to that of Stepanchikova and Kolonin (1999). Individual ion activity coefficients were calculated using the extended Debye-Hückel equation (Helgeson, 1969):

$$\log \gamma_n = \frac{A \cdot [z_n]^2 \cdot \sqrt{I}}{1 + B \cdot a \cdot \sqrt{I}} + b \cdot I \quad (5)$$

where I varied from 0.08 to 0.3.

Following Gammons et al. (1996), values for a (distance of closest approach) for H^+ and Cl^- were taken from Kielland (1937), and those for neodymium species were set to 9 \AA . The

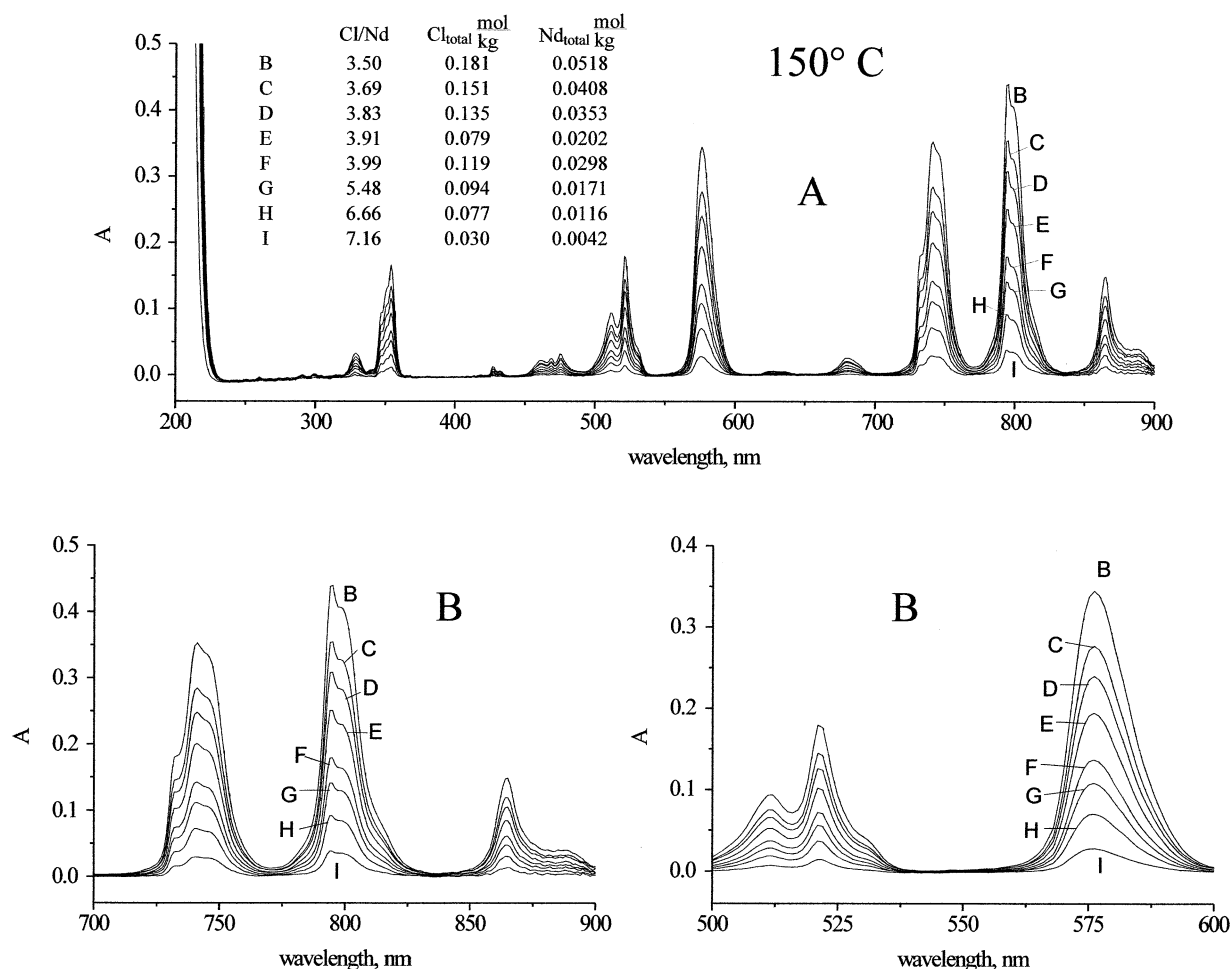


Fig. 4. (A) Examples of the selected spectra at 150°C for a set of solutions with variable Nd:Cl ratios. (B) Enlargements of parts of the spectra shown in (A).

coefficients for the Debye-Hückel equation were taken from Helgeson (1969) and Helgeson et al. (1981), using HCl as the model solute. The fact that values of Debye-Hückel parameters and models employed in this study are the same as those used by Gammons et al. (1996) allows direct comparison of the formation constants obtained in the two studies. The small difference between our activity model and that of Stepanchikova and Kolonin (1999) (they used different values for the distances of closest approach) is not considered sufficient to explain the appreciable differences in the values of β_1 obtained in their study from those reported here (see below).

Our calculations were performed with initial guesses for the values of β_1 and β_2 constants (see Eqn. 2 and 3) deliberately chosen to be significantly different from the values obtained by Stepanchikova and Kolonin (1999) (β_1) and Gammons et al. (1996) and involved several cycles of iteration, which minimized U (Eqn. 4) with respect to β_1 and β_2 . Each of these iteration cycles incorporated a further internal cycle of iteration in which U (Eqn. 4) was minimized with respect to the molar extinction coefficients of the Nd species. The absorption term for the chloride ion was calculated using molar extinction coefficients obtained in neodymium-free solutions of HCl. Two independent sets of calculation were performed, one involving

experimentally determined molar extinction coefficients for Nd^{3+} , which were held constant in the optimization procedure, and the other in which these coefficients were optimized during the minimization. There were no significant differences in the values of the formation constants obtained using these two different methods of calculation. These values are summarized in Table 2. Unfortunately, stable solutions were not obtained for $\beta_1^{25^\circ\text{C}}$ and $\beta_2^{100^\circ\text{C}}$. Their values varied with the initial guesses, indicating that there are several possible solutions for the model investigated. We assumed that low concentrations of NdCl_2^+ and NdCl^+ at the above two temperatures and the resulting low intensities of the corresponding absorption bands led to unstable solutions for the formation constants. The values of $\log \beta_1$ (0.28) and $\log \beta_2$ (0.1) reported in Table 2 for 25 and 100°C, respectively, represent the solutions closest to the values of Gammons et al. (1996), Mironov et al. (1982), and Millero (1992). They are nevertheless considered unreliable and should be used with caution.

To estimate the errors associated with the derivation of the formation constants, we modeled the distribution of the overall error for the treatment of the spectra as a function of β_1 and β_2 for each of the isotherms investigated. The overall error was calculated using the following relationship:

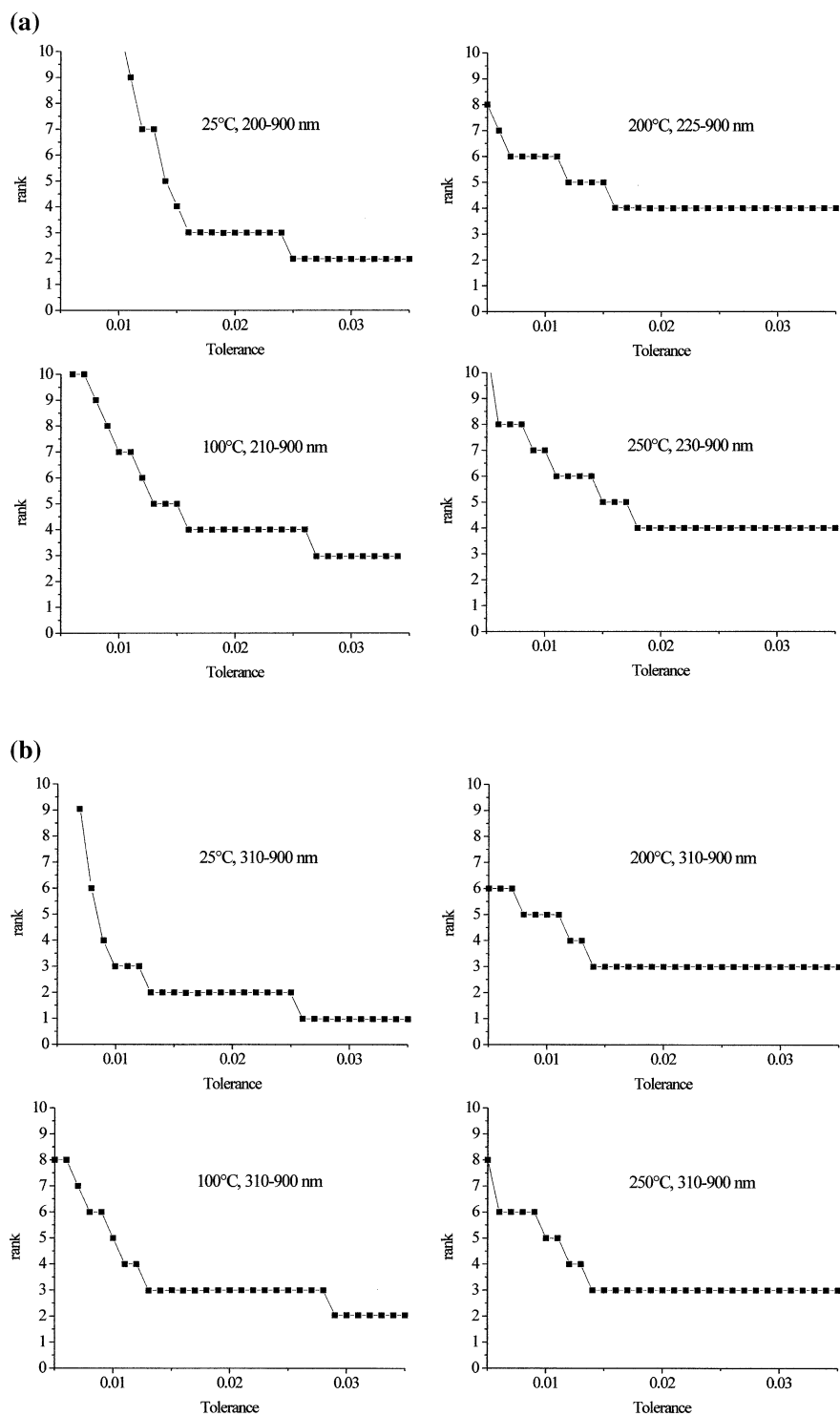


Fig. 5. (A) The results of rank calculations for the absorbance matrix. The rank represents the number of independent linear equations in the absorption matrix, which, effectively, is the number of absorbing species (see explanation in the text). (B) The results of rank calculations for the absorbance matrix for wavelengths of 310 to 900 nm.

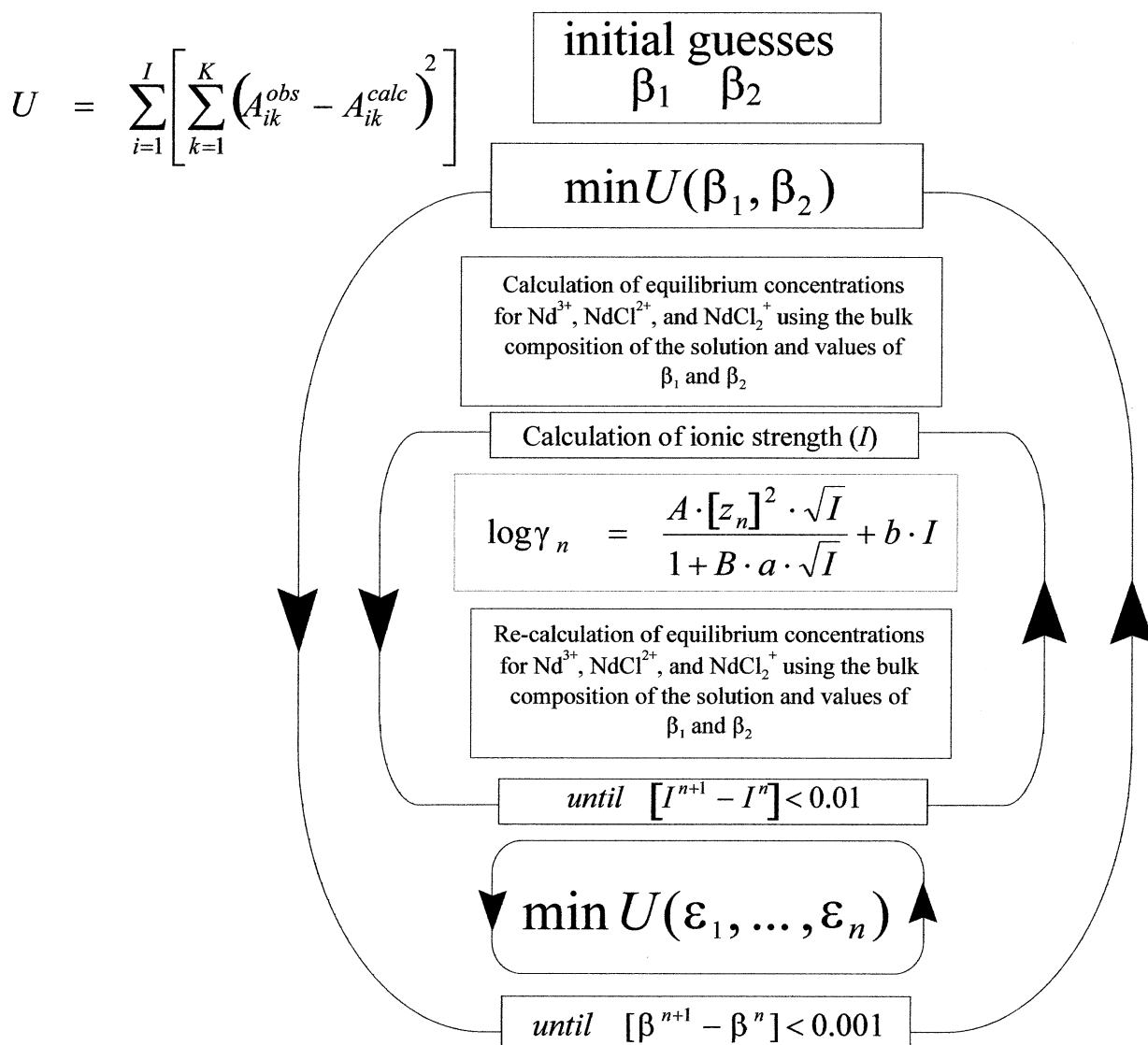


Fig. 6. A schematic block diagram describing the algorithm used to calculate the values of the formation constants β_1 and β_2 .

$$\text{Overall Error} = 100 \cdot \sqrt{\frac{\sum_{i=1}^I \left[\sum_{k=1}^K (A_{ik}^{obs} - A_{ik}^{calc})^2 \right]}{\sum_{i=1}^I \left[\sum_{k=1}^K A_{ik}^{obs^2} \right]}}, \quad (6)$$

where I is the total number of wavelengths at which measurements were made, and K is the number of solutions (see Eqn. 4) (e.g., Liu et al., 2001). Examples of these distributions for 100 and 200°C are shown in Figures 7a and 7b, respectively, as “maps” of the error surface in $\log \beta_1 - \log \beta_2$ coordinates. As can be seen in Figure 7, the optimized values of the formation constants correspond to the “deepest” depressions in the maps. On each of the maps, we show isolines representing the accuracy in the measurement of the spectra. The accuracy was

calculated from the values of the tolerance, which were obtained in the rank calculations (see speciation model) using the following relationship:

$$\text{Accuracy} = 100 \cdot \sqrt{\frac{\sum_{i=1}^I \left[\sum_{k=1}^K \text{tol}^2 \right]}{\sum_{i=1}^I \left[\sum_{k=1}^K A_{ik}^{obs^2} \right]}}, \quad (7)$$

where tol is the minimum tolerance required for the given speciation model. Projections of this isoline onto the $\log \beta_1$ and $\log \beta_2$ axes show the error in the derivation of the corresponding formation constant. It can be seen that at 100°C, the surface of errors has a minimum in the form of a long narrow valley with a flat bottom oriented parallel to the ordinate. From this

Table 2. Values of the formation constants for NdCl_2^{2+} and NdCl_2^+ obtained in this study. Parentheses indicate values not reliably determined (see text).

$T(^{\circ}\text{C})$	$\log \beta_1$	$\log \beta_2$
25	(0.28)	—
100	0.58 ± 0.16	(0.10)
125	0.84 ± 0.18	0.52 ± 0.24
150	1.22 ± 0.21	1.39 ± 0.22
175	1.69 ± 0.20	2.33 ± 0.20
200	2.25 ± 0.22	3.15 ± 0.18
225	2.83 ± 0.24	3.91 ± 0.19
250	3.4 ± 0.25	4.64 ± 0.21

diagram, it is evident that while the value of $\log \beta_1$ can be derived within a reasonable error (± 0.16 at this temperature), the error of derivation for $\log \beta_2$ is too large for the value of $\log \beta_2$ to be considered reliable.

5. DISCUSSION

5.1. Data Comparison

The values of β_1 reported above are identical within experimental error to the values recommended by Gammons et al. (1996) but differ substantially from those proposed by Stepanchikova and Kolonin (1999) (Tables 3 and 4, Fig. 8). As can be seen from Figure 8a, the values for β_1 are an order of magnitude lower than those of Stepanchikova and Kolonin (1999) at 100°C and an order of magnitude higher than their values at 250°C; the two data sets predict similar values at 175 to 180°C. This disagreement is due at least partly to differences in the chemical models employed in data reduction. The model employed in our study and that of Gammons et al. (1996) involved three Nd-bearing species (Nd^{3+} , NdCl_2^{2+} , and NdCl_2^+), whereas that of Stepanchikova and Kolonin (1999) involved only Nd^{3+} and NdCl_2^{2+} . Thus, at temperatures above 200°C, for which we interpret NdCl_2^+ to predominate, it was inevitable that the values of $\log \beta_1$ reported by Stepanchikova and Kolonin (1999) would be different from those reported here. However, we would have expected them to be higher, not lower, than our values. Similarly, we have no reasonable explanation for why their values are higher at low temperatures, considering that the speciation model employed in the two studies was effectively the same for these conditions.

The values of β_2 obtained in this study agree relatively well with those of Gammons et al. (1996), except at intermediate temperature; they reach a maximum difference of half an order of magnitude at 200°C (Fig. 8b).

It should be noted that the formation constants reported in this study were obtained for a total pressure of 50 ± 1 bars, whereas those of Stepanchikova and Kolonin (1999) and Gammons et al. (1996) represent the pressure of saturated water vapor. However, the differences in the values of the formation constants for most aqueous species do not exceed 0.05 log units because of these differences in pressure at the temperatures investigated. For example, the values of $\log \beta_1^{25^{\circ}\text{C}}$ for fluoride complexes of aluminum are 6.98 at saturated vapor pressure and 6.95 at 50 bars, and the values of $\log \beta_1^{250^{\circ}\text{C}}$ are 9.32 at saturated vapor pressure and 9.31 at 50 bars (Johnson et al., 1992). The differences in $\log \beta$ values for manganese chloride

Table 3. A comparison of the values of $\log \beta_1$ obtained in this study with those recommended by others authors. The data subtitled Haas et al. (1995) represent values calculated theoretically using Helgeson-Kirkham-Flowers model parameters, estimated in part from data of Wood (1990).

$T(^{\circ}\text{C})$	Our data	Gammons et al. (1996)	Stepanchikova and Kolonin (1999)	Haas et al. (1995)
25	(0.28)	0.06	—	0.304
100	0.58	0.66	1.43	0.920
125	0.84	—	—	1.133
150	1.22	1.31	1.67	1.359
175	1.69	—	—	1.599
200	2.25	2.17	2	1.858
225	2.83	—	—	2.140
250	3.4	3.22	2.45	2.456

are 0.04 and 0.06, respectively (Johnson et al., 1992). Thus, assuming that Nd-chloride complexes behave similarly, we can predict that the differences between the measurements made at saturated vapor pressure and at 50 bars would be indistinguishable within experimental error.

5.2. Comparison With Theoretical Predictions

The experimentally determined constants for reactions 2 and 3 were also compared with the corresponding constants calculated using the revised Helgeson-Kirkham-Flowers (HKF) equation of state parameters (Shock and Helgeson, 1988; Tanger and Helgeson, 1988; Shock et al., 1989, 1992) for NdCl_2^{2+} and NdCl_2^+ recommended by Haas et al. (1995). The parameters for Nd^{3+} and Cl^- were taken from Shock et al. (1989). As can be seen from Figures 8 and 9, the values of Haas et al. (1995) are also substantially different from those determined experimentally in this study and in the study of Gammons et al. (1996). Both calculated constants (β_1 and β_2) predict significantly weaker complexation at elevated temperatures, and their values differ by 1 order of magnitude at 250°C from the values determined experimentally. On the other hand, the stability of NdCl_2^+ is overestimated at temperatures below 150°C.

To fit our data to the HKF model, we calculated the apparent Gibbs free energies for NdCl_2^{2+} and NdCl_2^+ from the experimentally derived constants and used the free energies for Nd^{3+} and Cl^- reported by Shock et al. (1989). The calculations of the apparent free energies for NdCl_2^{2+} and NdCl_2^+ were performed using the HCh software package (Shvarov and Bastrakov, 1999), which employs the same algorithm as SUPCRT92 (Johnson et al., 1992) and thus is fully compatible with the revised HKF model. The data were fitted to the HKF model using a weighted least squares method to minimize the difference between the calculated Gibbs free energies and the corresponding values from the experimental data. These calculations were made using the UT-HEL code, which is part of the HCh package. The HKF model parameters recommended by Haas et al. (1995) were used as initial guesses in the calculations. Because no experimental information is available on the pressure dependence of the stability of Nd-Cl species, only ΔG_{298} , S_{298} , and c_1 parameters were estimated. The results of these calculations are summarized in Table 5; the formation constants calculated using the above parameters are illustrated

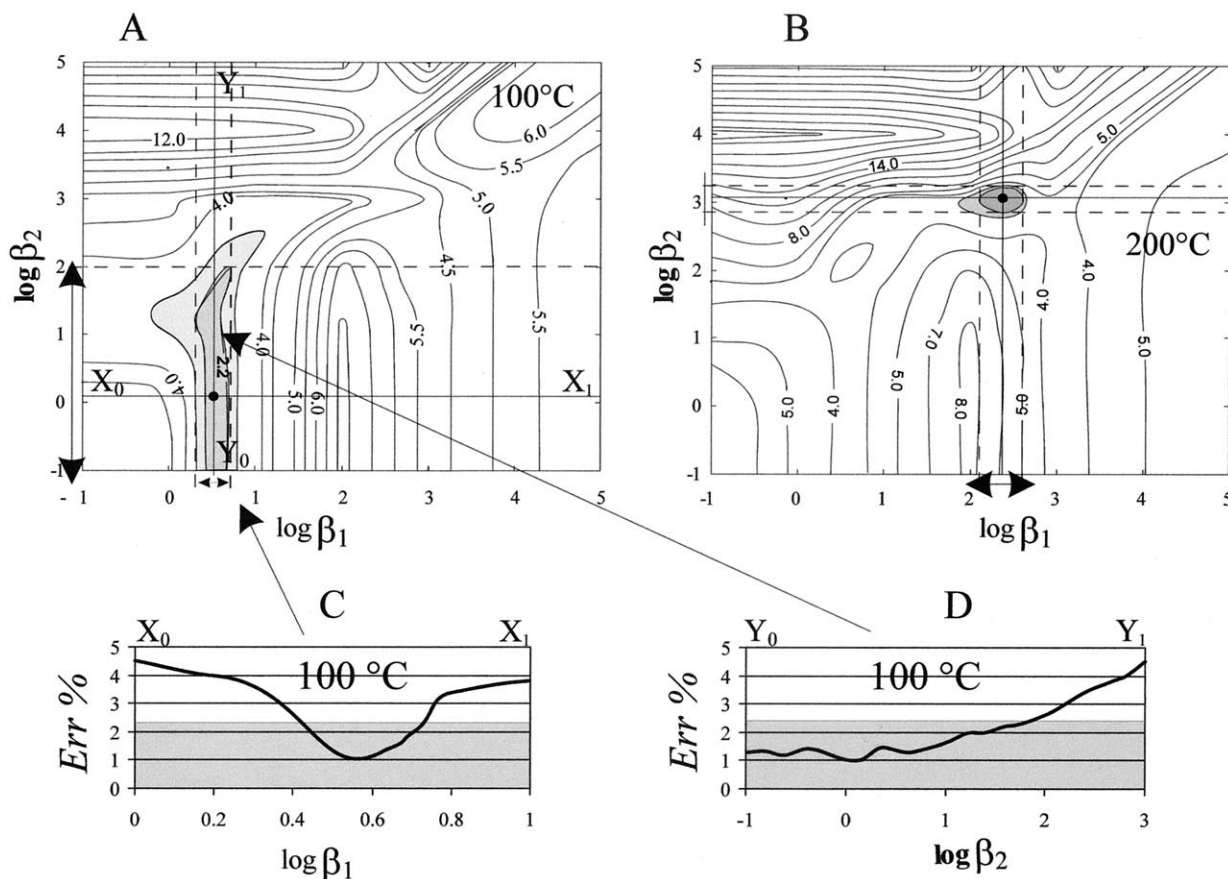


Fig. 7. The distribution of the overall errors for the treatment of the spectra as a function of β_1 and β_2 at (A) 100°C and (B) 200°C. The gray color represents areas where an accurate description of the spectra requires a precision higher than that of the experimental method. Projections of these areas onto the $\log \beta_1$ and $\log \beta_2$ axes show the errors associated with the derivation of the corresponding formation constant.

in Figure 9. It should be noted that although the calculated formation constants compare well with those determined experimentally, the absolute values of the HKF parameters are much larger than those estimated by Haas et al. (1995) for REE complexes. This may indicate inaccuracies in the accepted values of the standard thermodynamic properties for Nd^{3+} , from which the apparent free energies for NdCl_2^{2+} and NdCl_2^+ were calculated. The possibility of such inaccuracy has been discussed by other researchers who have investigated the aque-

ous speciation of the REEs. For example, Diakonov et al. (1998) found that the calculated solubility of $\text{Nd}(\text{OH})_3$ at 298.15 K was >1.5 orders of magnitude higher than that determined from experimental data. This therefore suggests that the values of the standard thermodynamic properties for the Nd^{3+} ion need to be reexamined.

Unfortunately, we are unable to evaluate the properties of Nd^{3+} on the basis of our experimental data or even estimate the extent of any error. However, if there are errors in the thermodynamic data for Nd^{3+} , they do not affect our estimates of the relationships among the Nd species studied in our experiments. Because the constants determined in our experiments are very similar to those recommended by Gammons et al. (1996), the species distribution is also very similar to that predicted by their model. At 25°C and low chloride concentrations, the free ion, Nd^{3+} , dominates in the solutions. However, when temperature increases, NdCl_2^{2+} takes over as the dominant neodymium species (at 100 to 150°C, depending on Cl^- concentration). At temperatures of 200 to 250°C the dominant neodymium species in Cl-bearing solutions is NdCl_2^+ . Despite the fact that neodymium forms only weak complexes with chloride at 25°C, the stability of these species increases sharply with temperature and at 250°C is 3 to 4 orders of magnitude higher.

Table 4. A comparison of the values of $\log \beta_2$ obtained in this study with those recommended by Gammons et al. (1996) and Haas et al. (1995). The latter are calculated values based on Helgeson-Kirkham-Flowers model parameters (Haas et al., 1995).

$T(^{\circ}\text{C})$	Our data	Gammons et al. (1996)	Haas et al. (1995)
100	(0.10)	0.13	0.893
125	0.52	—	1.201
150	1.38	1.08	1.530
175	2.33	—	1.886
200	3.15	2.52	2.277
225	3.91	—	2.713
250	4.64	4.45	3.216

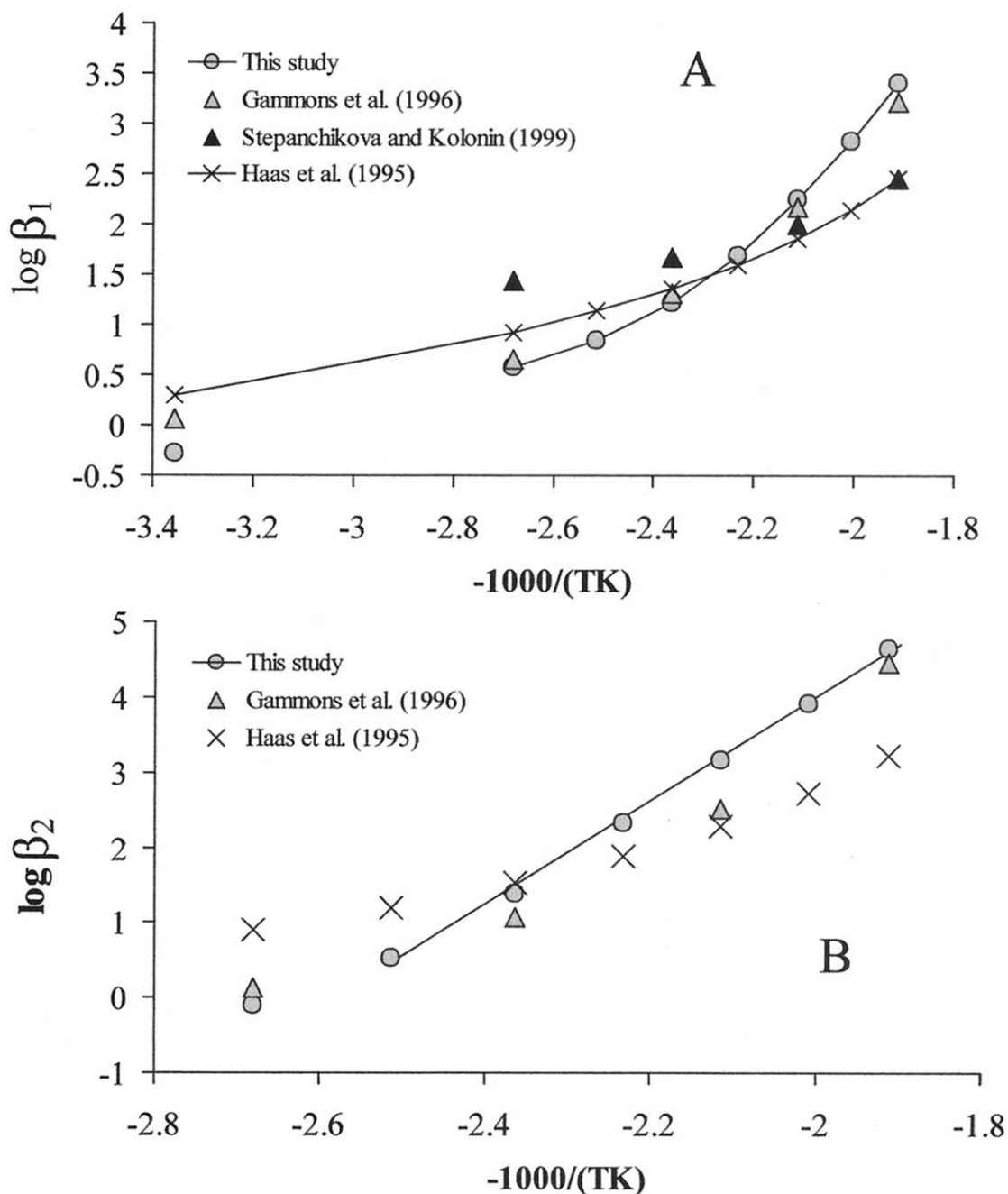


Fig. 8. A comparison of the values of (A) β_1 and (B) β_2 obtained in this study with those published by Stepanchikova and Kolonin (1999) and Gammons et al. (1996). Also shown are the constants calculated using the Helgeson-Kirkham-Flowers model parameters for Nd^{3+} , NdCl^{2+} , and NdCl_2^+ recommended by Haas et al. (1995).

In principle, it should be possible to use our data to evaluate the capacity of hydrothermal fluids to mobilize Nd. However, because this mobility is determined partly by the stability of the Nd^{3+} ion, reliable thermodynamic data are required for the latter, and as discussed above, the accepted data may be incorrect. This point is illustrated by considering the concentrations of Nd in hydrothermal solutions in equilibrium with monazite ($[\text{La,Ce,Nd}]\text{PO}_4$). For example, Wood and Williams-Jones (1994), using the thermodynamic data for aqueous species of Vieillard and Tardy (1984) and the formation constants pre-

dicted by Wood (1990) for Nd-Cl species, estimated a maximum Nd concentration of 1 ppb at 300°C for a typical seafloor hydrothermal vent fluid ($\Sigma\text{Cl} = 0.6 \text{ mol/L}$). Using the same standard thermodynamic data and formation constants for NdCl^{2+} and NdCl_2^+ extrapolated from Table 2, saturation with respect to Nd-monazite occurs at a Nd concentration of 2 ppb for the same conditions (this value is indistinguishable from that reported by Gammons et al., 1996). By contrast, the above calculation performed using the data from Shock et al. (1989) or Shock and Helgeson (1988) predicts concentrations several

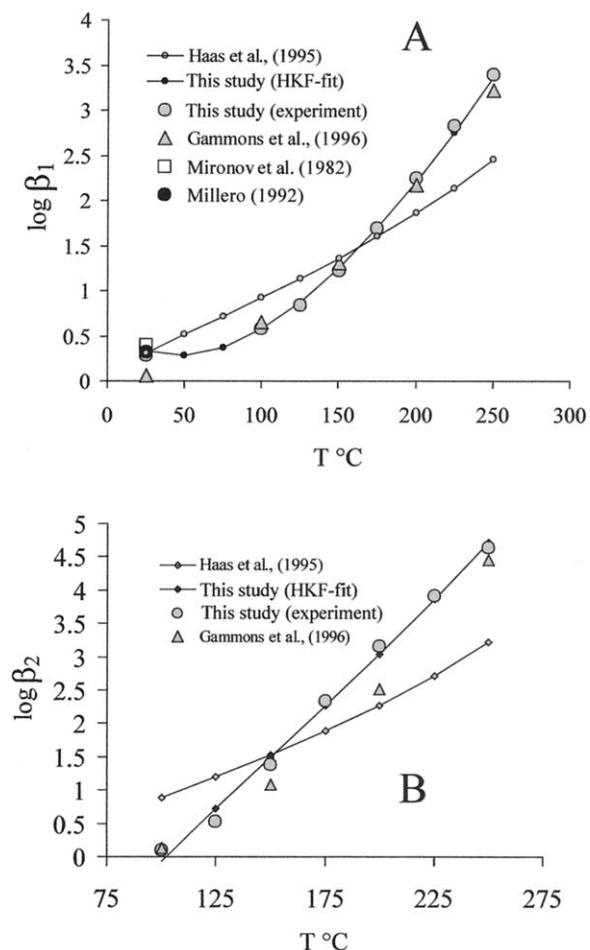


Fig. 9. Formation constants calculated using the Helgeson-Kirkham-Flowers (HKF) model parameters for Nd^{3+} , NdCl_2^{2+} , and NdCl_2^+ recommended by Haas et al. (1995) and those extracted from the results of our experiments. The calculated values are compared with those determined experimentally in this study and by Gammons et al. (1996).

orders of magnitude lower. These calculations also suggest that the stability of Nd chloride complexes is too low to explain the enrichments in Nd of hundreds of parts per million, which have

Table 5. A comparison of Helgeson-Kirkham-Flowers (HKF) model parameters for NdCl_2^{2+} and NdCl_2^+ proposed in this study with HKF parameters recommended by Haas et al. (1995).

	NdCl_2^{2+}		NdCl_2^+	
	Haas et al. (1995)	This study	Haas et al. (1995)	This study
ΔG_{298}	-223400	-219893	-192400	-192443
S_{298}	-5.9	15.233	-22.7	-41.95
a_1^*E1	2.3933	2.3933	-0.6746	-0.6746
a_2^*E-2	-1.9354	-1.9354	-9.4228	-9.4228
a_3	6.5057	6.5057	9.439	9.439
a_4^*E-4	-2.6989	-2.6989	-2.3894	-2.3894
c_1	-9.179	24.8303	8.4972	102.1569
c_2^*E-4	-10.414	-10.414	-6.7094	-6.7094
ω^0^*E-5	0.6388	0.6388	1.4006	1.4006
Z	1	1	2	2

been reported for alteration zones around volcanogenic massive sulfide deposits, i.e., paleo seafloor hydrothermal systems (MacLean, 1988; Schandl and Gorton, 1991). It should be noted, however, that this conclusion ignores errors related to the quality of thermodynamic data available for monazite and paucity of data for aqueous species and ion pairs involving phosphate, for which there are no data. Nevertheless, it does seem likely that other ligands probably play a more important role in the hydrothermal transport of Nd than chloride.

6. CONCLUSIONS

The experimental data obtained spectrophotometrically in this study confirm a chemical model of neodymium speciation proposed earlier by Gammons et al. (1996) based on solubility experiments. Chloride-bearing aqueous solutions of neodymium contain at least three Nd species: Nd^{3+} , NdCl_2^{2+} , and NdCl_2^+ . The values of the first formation constant (β_1) are in near perfect agreement with those recommended by Gammons et al. (1996), and those for the second formation constant (β_2) also agree reasonably well. By contrast, there is little agreement with Stepanchikova and Kolonin (1999) in respect either to the chemical model employed or to the values of the formation constants reported.

At 25°C and low chloride concentrations, Nd^{3+} is the dominant form of neodymium in aqueous solutions. However, with increasing temperature, the speciation changes, with NdCl_2^{2+} and NdCl_2^+ becoming dominant for a wide range of Cl concentrations. Moreover, the stability of both these species increases sharply with increasing temperature. Nevertheless, neodymium chloride complexes are not sufficiently stable to account for the relatively high mobility of Nd reported for natural systems.

Acknowledgments—This research was made possible through grants from the Natural Sciences and Engineering Research Council and FCAR to A. E. Williams-Jones and the assistance of T. Seward, O. Suleimenov (ETH, Zurich, Switzerland), and S. Kecani (McGill University, Montreal, Canada) in the design of the UV-visible cell used in the experiments. The authors are also grateful to T. Seward and O. Suleimenov for their advice on various aspects of the study. The manuscript benefited from reviews by C. Gammons and an anonymous *Geochimica et Cosmochimica Acta* reviewer.

Associate editor: L. G. Benning

REFERENCES

- Buhn B. and Rankin A. H. (1999) Composition of natural, volatile-rich Na-Ca-REE-Sr carbonatitic fluids trapped in fluid inclusions. *Geochim. Cosmochim. Acta* **63**, 3781–3797.
- Buhn B., Rankin A. H., Radtke M., Haller M., and Knochel A. (1999) Burbankite, a (Sr,REE,Na,Ca)-carbonate in fluid inclusions from carbonatite-derived fluids: Identification and characterization using laser Raman spectroscopy, SEM-EDX, and synchrotron micro-XRF analysis. *Am. Mineral.* **84**(7–8), 1117–1125.
- Carnall W. T. (1979) The absorption and fluorescence spectra of rare earth ions in solution. *Handb. Phys. Chem. Rare Earths*, **3**, 171–208.
- Choppin G. R., Kelly D. A., and Ward E. E. (1966) Effect of changes in the ionic medium on the stability constant of $\text{Eu}(\text{NO}_3)_2^+$. AEC Access. Nos. (ORO-1797-2).
- Dennis J. E. Jr. and Woods D. J. (1987) Optimization on microcomputers: The Nelder-Mead simplex algorithm. In: *New Computing*

- Environments: Microcomputers in Large-Scale Computing* (ed. A. Wouk), pp. 116–122. SIAM, Philadelphia, PA.
- Diakonov I. I., Tagirov B. R., and Ragnarsdottir K. V. (1998) Standard thermodynamic properties and heat capacity equations for rare earth element hydroxides. Part 1. La(OH)₃(s) and Nd(OH)₃(s). Comparison of thermochemical and solubility data. *Radiochim. Acta* **81**(2), 107–116.
- Dongarra J. J., Bunch J. R., Moler C. B., and Stewart G. W. (1979) LINPACK Users' Guide, SIAM, Philadelphia.
- Drew L. J., Oingrun M., and Weijun S. (1990) The Bayan Obo iron-rare-earth-niobium deposit, Inner Mongolia, China. *Lithos* **26**, 43–65.
- Gammons C. H., Wood S. A., and Williams-Jones A. E. (1996) The aqueous geochemistry of the rare earth elements and yttrium: VI. Stability of neodymium chloride complexes from 25 to 300°C. *Geochim. Cosmochim. Acta* **60**, 4615–4630.
- Gammons C. H., Wood S. A., and Youning L. (2002) Complexation of the rare earth elements with aqueous chloride at 200°C and 300°C and saturated water vapor pressure. In *Water-Rock Interaction, Ore Deposits, and Environmental Geochemistry: A Tribute to David A. Crerar*, Special Publication No. 7 (eds. R. Hellmann and S. A. Wood), pp. 191–207. The Geochemical Society, St. Louis, MO.
- Haas J. R., Shock E. L., and Sassani D. C. (1995) Rare earth elements in hydrothermal systems: Estimates of standard partial molal thermodynamic properties of aqueous complexes of the rare earth elements at high pressures and temperatures. *Geochim. Cosmochim. Acta* **59**, 4329–4350.
- Helgeson H. C. (1969) Thermodynamics of hydrothermal systems at elevated temperatures and pressures. *Am. J. Sci.* **267**(7), 729–804.
- Helgeson H. C., Kirkham D. H., and Flowers G. C. (1981) Theoretical prediction of the thermodynamic behavior of aqueous electrolytes at high pressures and temperatures: IV. Calculation of activity coefficients, osmotic coefficients, and apparent molal and standard and relative partial molal properties to 600°C and 5 kb. *Am. J. Sci.* **281**(10), 1249–1516.
- Johnson J. W., Oelkers E. H., and Helgeson H. C. (1992) SUPCRT 92: A software package for calculating the standard molal thermodynamic properties of minerals, gases, aqueous species, and reactions from 1 to 5000 bars and 0° to 1000°C. *Comput. Geosci.* **18**(7), 899–947.
- Kielland J. (1937) Individual activity coefficients of ions in aqueous solutions. *J. Am. Chem. Soc.* **59**, 1675–1678.
- Kotzian M., Fox T., and Roesch N. (1995) Calculation of electronic spectra of hydrated Ln(III) ions within the INDO/S-CI approach. *J. Phys. Chem.* **99**(2), 600–605.
- Kwak T. A. P. and Abeyasinghe P. B. (1987) Rare earth and uranium minerals present as daughter crystals in fluid inclusions, Mary Kathleen U-REE skarn, Queensland, Australia. *Mineral. Mag.* **51**(363), 665–670.
- Liu W., McPhail D. C., and Brugger J. (2001) An experimental study of copper(I)-chloride and copper(I)-acetate complexing in hydrothermal solutions between 50°C and 250°C and vapor-saturated pressure. *Geochim. Cosmochim. Acta* **65**, 2937–2948.
- MacLean W. H. (1988) Rare earth mobility at constant inter REE ratios in the alteration zone at the Phelps Dodge massive sulfide deposit, Mattagami, Quebec. *Mineral. Deposita* **23**, 231–238.
- Millero F. J. (1992) Stability constants for the formation of rare earth inorganic complexes as a function of ionic strength. *Geochim. Cosmochim. Acta* **56**, 3123–3132.
- Mironov V. E., Avramenko N. I., Kopyrin A. A., Blokhin V. V., Eike M. Yu., and Isaev I. D. (1982) Thermodynamics of the formation of monochloride complexes of rare earth metals in aqueous solutions. *Koord. Khim.* **8**(5), 636–638.
- Nelder J. A. and Mead R. (1965) A simplex method for function minimization. *Comput. J.* **7**, 308–313.
- Olivo G. R. and Williams-Jones A. E. (1999) Hydrothermal REE-rich eudialyte from the Pilanesberg Complex, South Africa. *Can. Mineral.* **37**(3), 653–663.
- Salvi S. and Williams-Jones A. E. (1990) The role of hydrothermal processes in the granite-hosted zirconium, yttrium, REE deposit at Strange Lake, Quebec/Labrador: Evidence from fluid inclusions. *Geochim. Cosmochim. Acta* **54**, 2403–2418.
- Schandl E. S. and Gorton M. P. (1991) Postore mobilization of rare earth elements at Kidd Creek and other Archean massive sulfide deposits. *Econ. Geol.* **86**, 1546–1553.
- Shock E. L. and Helgeson H. C. (1988) Calculation of the thermodynamic and transport properties of aqueous species at high pressures and temperatures: Correlation algorithms for ionic species and equation of state predictions to 5 kb and 1000°C. *Geochim. Cosmochim. Acta* **52**, 2009–2036.
- Shock E. L., Helgeson H. C., and Sverjensky D. A. (1989) Calculation of the thermodynamic and transport properties of aqueous species at high pressures and temperatures: Standard partial molal properties of inorganic neutral species. *Geochim. Cosmochim. Acta* **53**, 2157–2183.
- Shock E. L., Oelkers E. H., Johnson J. W., Sverjensky D. A., and Helgeson H. C. (1992) Calculation of the thermodynamic properties of aqueous species at high pressures and temperatures: effective electrostatic radii, dissociation constants and standard partial molal properties to 1000°C and 5 kbar. *J. Chem. Soc., Faraday Trans.* **88**(6), 803–826.
- Shvarov Y., Bastrakov E. (1999) *HCh: A Software Package for Geochemical Equilibrium Modelling, User's Guide*. Australian Geological Survey Organization Record.
- Smith M. P. and Henderson P. (2000) Preliminary fluid inclusion constraints on fluid evolution in the Bayan Obo Fe-REE-Nb deposit, Inner Mongolia, China. *Econ. Geol.* **95**(7), 1371–1388.
- Stepanchikova S. A. and Kolonin G. R. (1999) Spectrophotometric study of complexation of neodymium in chloride solutions at temperatures up to 250°C. *Zh. Neorg. Khim.* **44**(10), 1744–1751.
- Suleimenov O. M. and Seward T. M. (2000) Spectrophotometric measurements of metal complex formation at high temperatures: The stability of Mn(II) chloride species. *Chem. Geol.* **167**(1–2), 177–192.
- Tanger J. C. IV and Helgeson H. C. (1988) Calculation of the thermodynamic and transport properties of aqueous species at high pressures and temperatures: Revised equations of state for the standard partial molal properties of ions and electrolytes. *Am. J. Sci.* **288**(1), 19–98.
- Viellard P. and Tardy Y. (1984) Thermochemical properties of phosphates. In *Phosphate Minerals* (eds. J. O. Nriagu and P. B. Moore), pp. 171–198. Springer, New York.
- Vinokurov S. F., Gorshkov A. I., Kovalenker V. A., and Magazina L. O. (1999) Lanthanides in quartz from hydrothermal gold ore deposits: Forms of occurrence. *Dokl. Akad. Nauk.* **367**(2), 234–237.
- Vogel L. M. (1986) *Spectroscopic Studies of Iron II, Iron III, and Manganese II Chlorocomplexes in Hot Aqueous Solutions*. Ph.D. thesis, Princeton University.
- Williams-Jones A. E., Samson I. M., and Olivo G. R. (2000) The genesis of hydrothermal fluorite-REE deposits in the Gallinas Mountains, New Mexico. *Econ. Geol.* **95**(2), 327–341.
- Wood S. A. (1990) The aqueous geochemistry of the rare-earth elements and yttrium. 2. Theoretical predictions of speciation in hydrothermal solutions to 350°C at saturation water vapor pressure. *Chem. Geol.* **88**(1–2), 99–125.
- Wood S. A. and Williams-Jones A. E. (1994) The aqueous geochemistry of the rare-earth elements and yttrium 4. Monazite solubility and REE mobility in exhalative massive sulfide-depositing environments. *Chem. Geol.* **115**, 47–60.
- Wood S. A. and Ricketts A. (2000) Allanite-(Ce) from the Eocene Casto Granite, Idaho: Response to hydrothermal alteration. *Can. Mineral.* **38**(1), 81–100.
- Wood S. A., Wesolowski D. J., and Palmer D. A. (2000) The aqueous geochemistry of the rare earth elements IX. A potentiometric study of Nd³⁺ complexation with acetate in 0.1 molal NaCl solution from 25°C to 225°C. *Chem. Geol.* **167**(1–2), 231–253.